Communication

Hybrid Method of Artificial Neural Network and Simulated Annealing Algorithm for Optimizing Wideband Patch Antennas

Yejun He, Jinhua Huang, Wenting Li, Long Zhang, Sai-Wai Wong, and Zhi Ning Chen

***Abstract*— In order to design the wideband patch antenna, a hybrid method based on the artificial neural network (ANN) and the simulated annealing (SA) algorithm is proposed in this communication. The ANN is employed to describe the nonlinear relationship between the geometric parameters and the *S*-parameters of the antenna. The ANN is trained by the dataset obtained from the high-frequency structure simulator (HFSS). More importantly, the dataset is divided into three groups according to their own characteristics so that the ANN can be trained faster and better. The SA is employed to broaden the bandwidth of the patch antenna with the required center frequency. Then three wideband patch antennas with different center frequencies are designed to demonstrate the feasibility of the proposed method. Several slots are added to the patch to achieve the wide bandwidth. The results prove that the proposed method can obtain the wideband patch antenna quickly and efficiently.**

***Index Terms*— Artificial neural network (ANN), simulated annealing (SA) algorithm, wideband antenna.**

I. Introduction

With the rapid development of the information technology, spectrum resources are increasingly becoming scarce. As an important part of the communication system, wideband antennas are becoming more and more demanding [1]. In general, the design of the wideband antenna is more time-consuming than that of the narrowband antenna. To speed up the design, many methods such as using parametric study [2], applying various optimization algorithms [3], [4], and employing the artificial neural network (ANN) [5], [6] have been proposed.

As a powerful method, the ANN can learn the complex nonlinear relationship between the input and output after being trained by the dataset. It has contributed greatly to modeling microwave filters [7], power amplifiers [8], [9], transistors [10], and antenna designs [11], [12], [13], [14]. The ANN can greatly accelerate the speed of antenna optimization. Therefore, the antenna design based on the ANN has received more and more attention.

Manuscript received 8 April 2023; revised 17 September 2023; accepted 10 October 2023. Date of publication 14 November 2023; date of current version 9 February 2024. This work was supported in part by the National Key Research and Development Program of China under Grant 2023YFE0107900; in part by the National Natural Science Foundation of China under Grant 62101341 and Grant 62071306; and in part by the Shenzhen Science and Technology Program under Grant 20200810131855001, Grant JCYJ20200109113601723, Grant JSGG20210420091805014, and Grant JSGG20210802154203011. *(Corresponding author: Wenting Li.)*

Yejun He, Jinhua Huang, Wenting Li, Long Zhang, and Sai-Wai Wong are with the State Key Laboratory of Radio Frequency Heterogeneous Integration, Sino-British Antennas and Propagation Joint Laboratory, Guangdong Engineering Research Center of Base Station Antennas, Shenzhen Key Laboratory of Antennas and Propagation, College of Electronics and Information Engineering, Shenzhen University, Shenzhen 518060, China (e-mail: heyejun@126.com; 1493107204@qq.com; w.li@szu.edu.cn; long.zhang@szu.edu.cn; wsw@szu.edu.cn).

Zhi Ning Chen is with the Department of Electrical and Computer Engineering, National University of Singapore, Singapore 117583 (e-mail: eleczn@nus.edu.sg).

Color versions of one or more figures in this communication are available at https://doi.org/10.1109/TAP.2023.3331249.

Digital Object Identifier 10.1109/TAP.2023.3331249

The ANN can predict the electromagnetic (EM) responses of the antenna accurately after it is well trained [15], [16]. In [17], a method with the ANN for array synthesis is proposed, where two serial ANNs are employed. One ANN is used as an encoder and the other is used as a decoder to realize the synthesis of the beam pattern for the linear array. Xiao et al. [18] utilize the combination of the ANN and the data classification technology to improve the performance of the antenna.

In addition to the above applications, the inverse problems of the antenna design could also be solved by the ANN [19], [20]. The EM responses of the antenna are fed into the ANN, and the geometric parameters could be output by the ANN. In [21], an ANN inverse model is established, in which the EM field intensity is the input, while the output is the radius of the loop antenna. A multibranch ANN is proposed to improve the performance of antenna arrays in [22]. The dataset is divided into different groups by judging the monotonicity of the data for solving the nonuniqueness problem, and each group is employed to train each branch.

In this communication, a hybrid method applying the combination of the ANN and the simulated annealing (SA) algorithm to design a wideband patch antenna is proposed. The dataset is employed to train the ANN which is obtained from the high-frequency structure simulator (HFSS). The input of the ANN is geometric parameters while the output is *S*-parameters. A trained ANN can describe the relationship between the geometric parameters and the EM responses of the antenna. Additionally, the ANN is called by the SA algorithm to calculate the cost function. Compared to the traditional optimization algorithm, the proposed method does not need to call the EM simulation repeatedly. As a result, it can speed up the design of the antenna, which requires only a small amount of human resources and can reduce the workload of the designer greatly. More importantly, the characteristic of the dataset is analyzed, and the dataset is separated into three subsets to train the ANN. In this way, the ANN can be trained better and faster. The bandwidth and center frequency of the antennas are optimized simultaneously. Three wideband patch antennas with different center frequencies are designed to verify the validity of the proposed method.

The communication is arranged as follows. The proposed method is introduced in detail in Section II. In Section III, the configuration of the antenna, the basic theory of the ANN, and the SA algorithm in the proposed method are introduced. In Section IV, the simulated and measured results of the three wideband patch antennas are given. Section V concludes the communication.

II. Proposed Hybrid Method

A. Artificial Neural Network

As a mathematical model for information processing, the ANN is inspired by a biological neural network. Although the ANN requires a large number of parameters and takes too long to learn, it has many advantages at the same time, for example, it can fully approximate complex nonlinear relations, has the ability of associative memory,

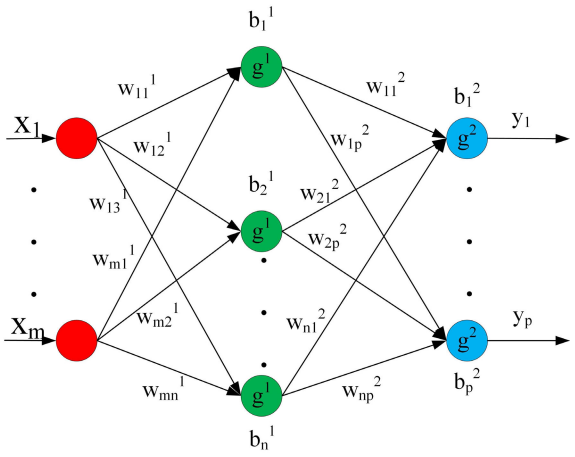

Fig. 1. ANN with the input layer, one hidden layer, and the output layer.

and has high classification accuracy. So the ANN is used to predict the relationship between the geometric parameters and EM responses of the antenna. The structure of a simple ANN with three layers is shown in Fig. 1. The ANN has one input layer, one hidden layer, and one output layer, and each layer has some neurons. The weights and thresholds are applied to connect neurons in adjacent layers. The activation functions could introduce nonlinear factors to the ANN so that it can solve nonlinear problems.

In the ANN, the geometric parameters of the antenna are the input, while EM responses of that are the output. x_i represents the ith geometric parameter ($1 \le i \le m$), and m is the number of input neurons. y_k indicates the kth EM response ($1 \le k \le p$). And p is the number of output neurons. y_k could be calculated by

$$y_k = g_2\left\{\sum_{j=1}^{n}\left[w_{jk}^2 g_1\left(\sum_{i=1}^{m} w_{ij}^1 x_i - b_j^1\right) - b_k^2\right]\right\} \tag{1}$$

where w_{ij}^1 represents the weight connecting the ith input neuron with jth hidden neuron, and w_{jk}^2 represents the weight which connects the jth hidden neuron with kth neuron in the output layer. b_j^1 indicates the threshold for the jth hidden neuron, while b_k^2 indicates the threshold for the kth output neuron. $g_1(x)$ and $g_2(x)$ are activation functions in the hidden layer and in the output layer, respectively. $g_1(x)$ and $g_2(x)$ can be expressed as

$$g_1(x) = \frac{1}{1+e^{-x}} \tag{2}$$

$$g_2(x) = x. \tag{3}$$

In training the ANN, the error is propagated back by the gradient descent method. During the backpropagation, the weights and thresholds of the ANN are updated continuously until the error is smaller than the set goal.

B. SA Algorithm

In the proposed method, the key of the SA algorithm is to construct the cost function which can be calculated with the trained ANN. The output of the ANN is taken as part of the cost function. The cost function C is given by

$$C = \omega\frac{f_1}{f_2} + (1-\omega)\left|\left(\frac{f_1+f_2}{2f_0} - 1\right)\right| \tag{4}$$

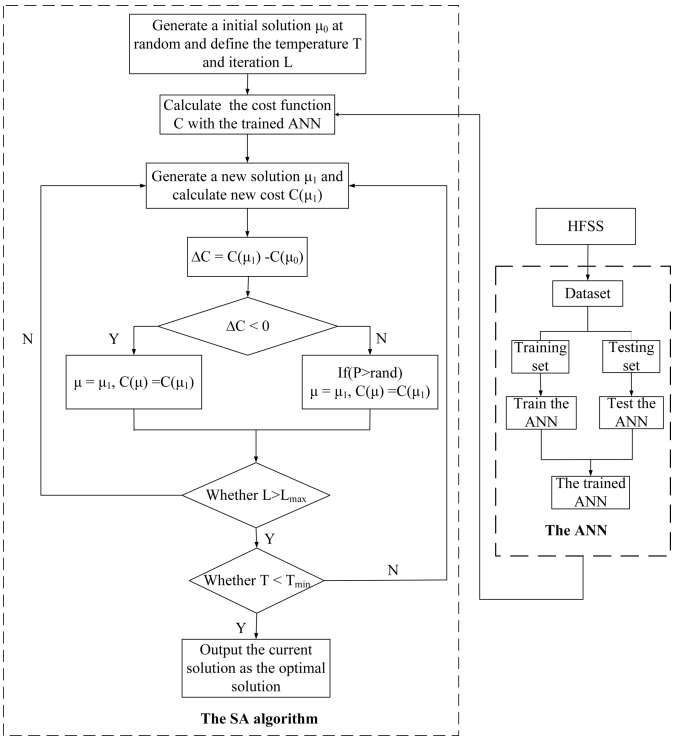

Fig. 2. Flowchart of the proposed hybrid method.

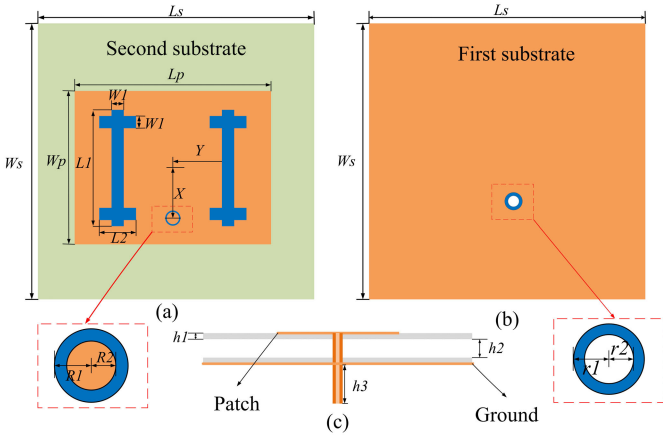

Fig. 3. Configuration of the antenna. (a) Top view. (b) Bottom view. (c) Side view. ($Ls = 52$, $Ws = 52$, $Lp = 26$, $W1 = 0.65$, $X = 5.2$, $R1 = 1.43$, $R2 = 1.3$, $r1 = 0.74$, $r2 = 0.32$, $h1 = 0.508$, $h2 = 1.71$, $h3 = 3.9$, unit: mm.)

where f_0 is the center frequency. The bandwidth is from f_1 to f_2, which are obtained from the ANN. Besides, ω is the weight of the bandwidth whose value is 0.02. In Fig. 2, the flowchart of the whole proposed hybrid method is given, which generally consists of the ANN and SA algorithm.

III. Wideband Patch Antenna Design

A. Structure of the Patch Antenna

The configuration of the patch antenna is given in Fig. 3. The antenna mainly consists of two substrates separated by an air gap. The first substrate is FR4 and the second substrate is RO4003. The patch is printed on the second substrate, and two symmetrical cross slots are added on the patch to make the bandwidth increased. The dimensions and placement of the slots and the width of the patch can be changed, while other parameters are fixed. Three wideband

TABLE I

DATASET OF THE PATCH ANTENNA (UNIT: MM)

Geometrical variables	Min	Max	Step
$L1$	1	15	2
$L2$	0.5	5	0.5
Y	1	9	2
Wp	18.2	23.4	2.6

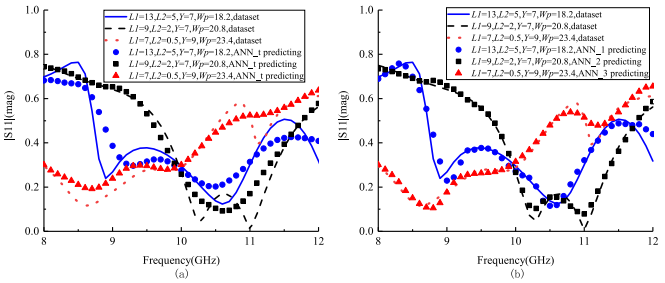

Fig. 4. Results of (a) ANN_t and of (b) ANN_1, ANN_2, ANN_3. Unit: mm.

antennas with different center frequencies are designed based on the patch antenna. The center frequency of the Antenna 1 is 9 GHz, while those of the Antenna 2 and Antenna 3 are 10 and 11 GHz, respectively.

B. Building the ANN to Predict EM Responses of the Patch Antenna

In order to predict the EM responses of the patch antenna, the ANN is built. $L1$, $L2$, Y, and Wp are fed into the ANN, and reflection coefficients are output by the ANN. The dataset containing 1200 sets which is produced by HFSS is used to train and test the ANN as shown in Table I. The dataset is divided into the training set (80%) and the testing set (20%) by random. All calculations are carried out by an Intel i7-10700 2.90 GHz machine with 32 GB RAM.

Since there are four geometric parameters and 41 output frequency points, The input layer of the ANN has four neurons, while the output layer owns 41 neurons. Each hidden layer has q neurons, and q is given by

$$q = \sqrt{a+b} + c \tag{5}$$

where a indicates the number of input neurons and b is that of output neurons. c is a random integer from 1 to 10. It can be calculated that q is from 8 to 17. q is determined to be 15 and the number of hidden layers is 3. The learning rate is determined to be 0.001. The mean square error (mse) which is utilized to assess the performance of the ANN is given by

$$\text{mse}\left(y, y'\right) = \frac{\sum_{i=1}^{N}\left(y_i - y_i'\right)^2}{N} \tag{6}$$

where y is the output of the testing set while y' represents the calculated value of the ANN. The testing set has N sets of data, where N is equal to 240.

At the beginning, 1200 sets are employed to train and test the ANN_t. However, the ANN_t could not be trained well. The testing results are shown in Fig. 4(a). It is observed that the results of the testing set do not match with the predictions of the ANN_t very well.

Then, the characteristic of the dataset is analyzed, as shown in Fig. 5. As can be seen from the figure, the dataset can be roughly divided into three blocks according to Wp. When $Wp = 18.2$ mm, it is represented by the circle. When $Wp = 20.8$ mm and $Wp = 23.4$ mm, they are represented by the cross and triangle, respectively.

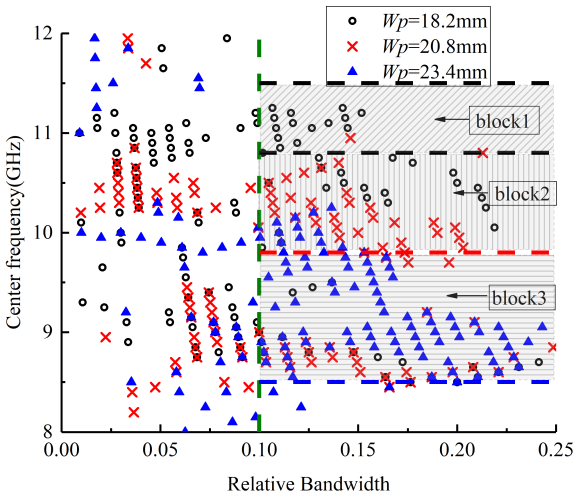

Fig. 5. Result of the data analysis.

TABLE II

TRAINING EPOCHS, TRAINING TIME, AND TESTING ERRORS OF THE ANN_T AND OF THE THREE ANNS

	Training epoch	Training time (minute)	Testing error
ANN_t	3000	50	9.87×10^{-4}
ANN_1	714	7	2.82×10^{-4}
ANN_2	668	6	3.89×10^{-4}
ANN_3	609	5	1.35×10^{-4}

TABLE III

FINAL VALUES OF THREE PARAMETERS OF THE THREE ANTENNAS

	$L1$ (mm)	$L2$ (mm)	Y (mm)	Wp (mm)	Simulated center frequency (GHz)
Antenna 1	9.30	3.12	10.70	18.2	8.93
Antenna 2	19.00	2.43	9.05	20.8	10.1
Antenna 3	11.86	6.45	11.69	23.4	11.1

In most situations, the center frequency f_0 of the antenna decreases as Wp increases which agrees with the theory of the patch antenna.

Therefore, the dataset is divided into three groups according to different values of Wp, and three sub-ANNs including ANN_1, ANN_2, and ANN_3 are built. The testing results of the three sub-ANNs are shown in Fig. 4(b). The results of the ANN_1, ANN_2, and ANN_3 are better than that of ANN_t. In Table II, the training epochs, training time, and testing errors of the ANN_t and the three ANNs are shown. It is observed that dividing the dataset into three groups and using three sub-ANNs can obtain better results, faster training speed, and higher accuracy. So, it can be seen that the preprocessing of data is beneficial to the learning of the ANN.

C. Applying the SA Algorithm to Broaden the Bandwidth of the Patch Antenna With the Required Center Frequency

After the building of the ANNs, the SA algorithm is applied to further broaden the bandwidth of the antennas with the required center frequency, because it can avoid the inverse problem in [20]. The required center frequency in the cost function is 9–11 GHz. The minimum value of the cost function is looked for until the SA algorithm stops running. Finally, the three groups of parameters found by the proposed method are shown in Table III. The simulated results and the calculated results by the proposed method are compared in Fig. 6, which reveals that the simulated results of the three antennas are in good agreement with the calculated results of the three antennas.

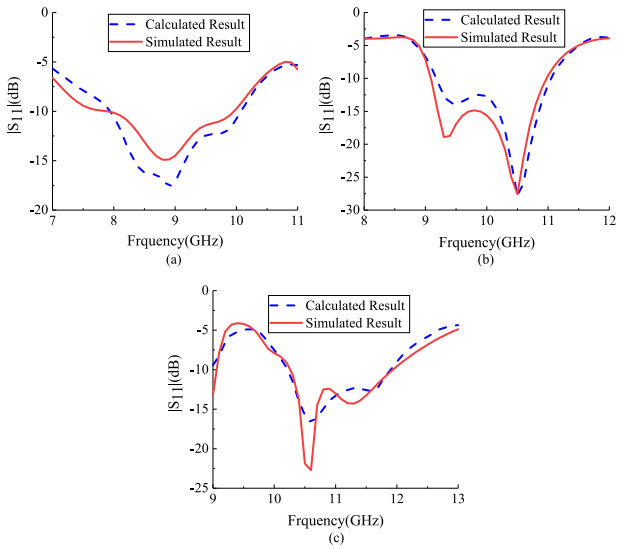

Fig. 6. Calculated and simulated $|S_{11}|$ of (a) Antenna 1, (b) Antenna 2, and (c) Antenna 3.

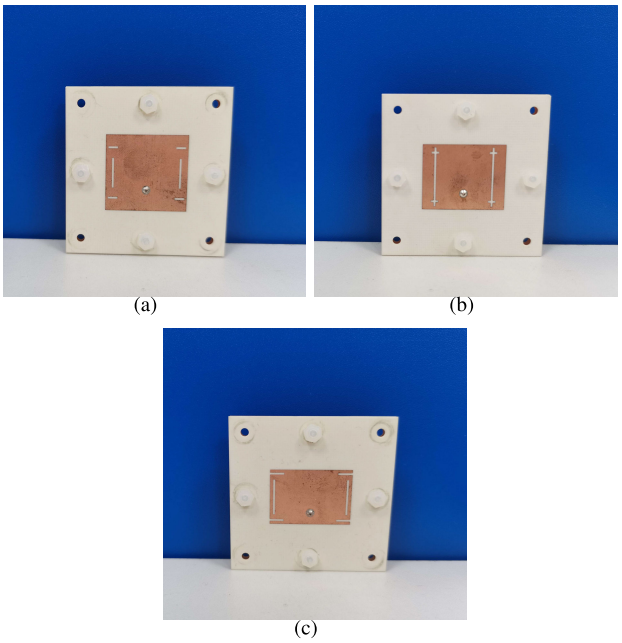

Fig. 7. Photographs of (a) Antenna 1, (b) Antenna 2, and (c) Antenna 3.

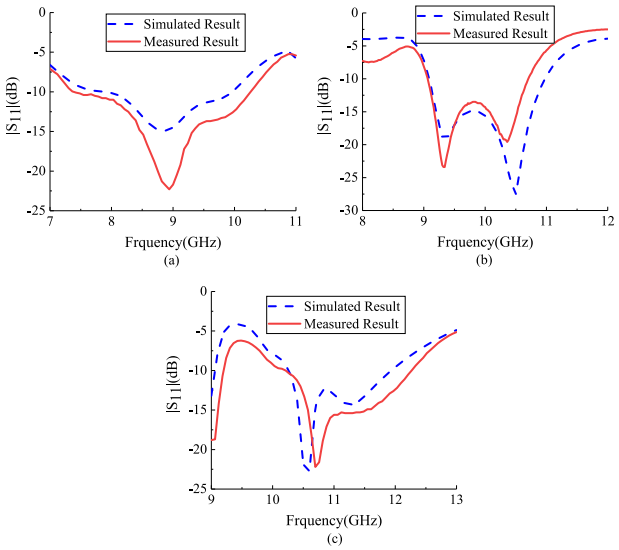

Fig. 8. Simulated and measured $|S_{11}|$ of (a) Antenna 1, (b) Antenna 2, and (c) Antenna 3.

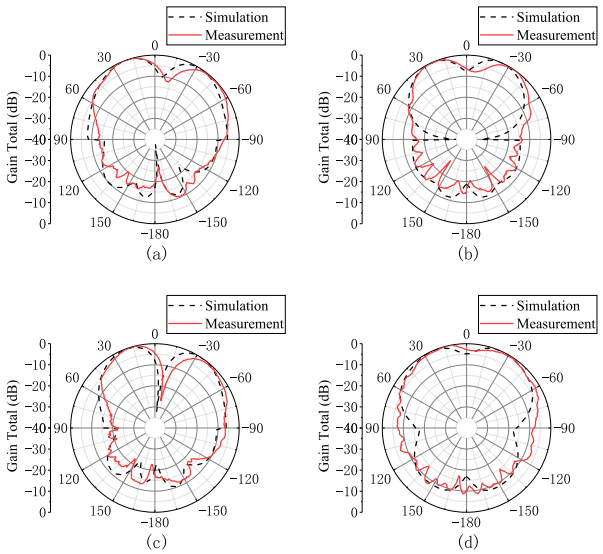

Fig. 9. Simulated and measured radiation patterns of Antenna 1. (a) 8.5 GHz (xoz plane). (b) 8.5 GHz (yoz plane). (c) 9 GHz (xoz plane). (d) 9 GHz (yoz plane).

TABLE IV

RUNNING TIME OF THE TRADITIONAL SA ALGORITHM, SVM, AND THE PROPOSED HYBRID METHOD

	Time
SA Algorithm	50.63 hours
SVM	7.5 hours (getting dataset) + 11.08 hours (modeling)
Proposed Hybrid Method	8.16 hours (getting dateset and modeling)+ 120 s (optimization)

The calculated working frequency band of Antenna 1 is from 7.95 to 10.05 GHz, and the center frequency is 9 GHz, while the simulated bandwidth is from 7.89 to 9.96 GHz, with a center frequency of 8.93 GHz. The calculated bandwidth of Antenna 2 is from 9.15 to 11.05 GHz, and the center frequency is 10.1 GHz. The simulated bandwidth of Antenna 2 is from 9.10 to 11.10 GHz, and the center frequency is 10.1 GHz. The calculated working frequency band of Antenna 3 is from 10.25 to 11.95 GHz, and the center frequency is 11.1 GHz, while the simulated bandwidth is from 10.26 to 11.94 GHz with the center frequency of 11.1 GHz.

The simulated time of the proposed antenna by HFSS is 90 s, whereas the simulated time of the proposed antenna together with the trained ANN is only 0.15 s. It takes about 2000 iterations to optimize the antenna by using the traditional SA algorithm where each iteration needs to call full-wave simulation, so it takes about 50 h in total. However, by using the proposed method, due to the parallel calculation method, four training samples can be calculated at the same time when the simulation software is run. It takes about 7.5 h to obtain the 1200 training samples. The total time is 8.16 h, including training and testing time of the ANN. And only 2 min is cost in the optimization of SA. Compared with the traditional SA algorithm calling EM simulations repeatedly during the antenna optimization, the proposed hybrid method can save time and improve the efficiency of antenna design. In addition, the proposed method is compared with the support vector machine (SVM) in terms of required time and prediction accuracy. SVM takes 11.08 h to train

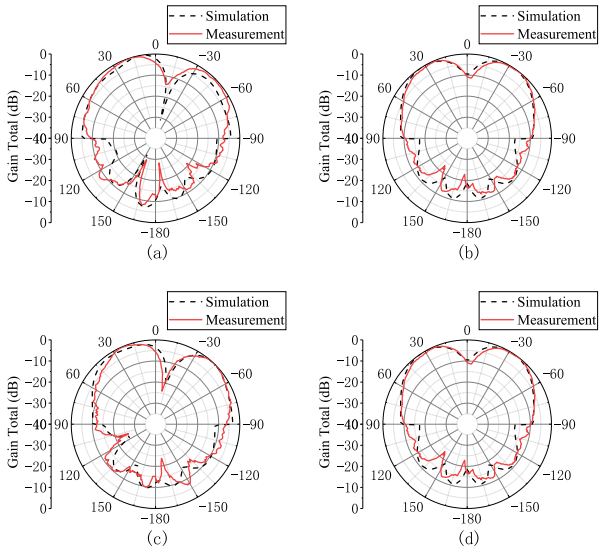

Fig. 10. Simulated and measured radiation patterns of Antenna 2. (a) 9.5 GHz (xoz plane). (b) 9.5 GHz (yoz plane). (c) 10 GHz (xoz plane). (d) 10 GHz (yoz plane).

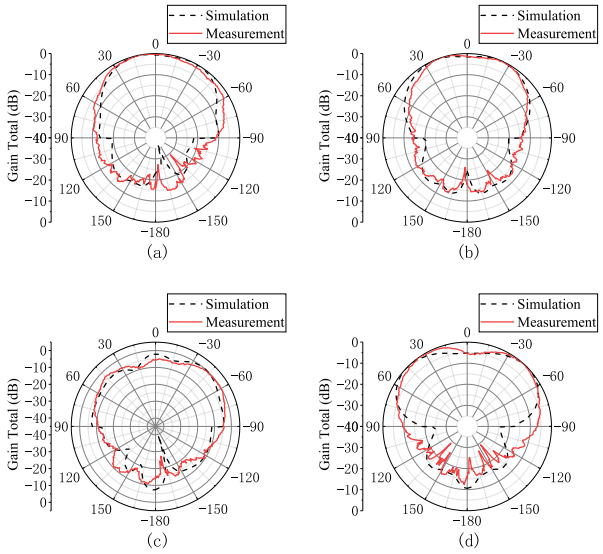

Fig. 11. Simulated and measured radiation patterns of Antenna 3. (a) 10.5 GHz (xoz plane). (b) 10.5 GHz (yoz plane). (c) 11 GHz (xoz plane). (d) 11 GHz (yoz plane).

and test the 1200 samples with a prediction error of 4.13×10^{-4}, while the proposed method takes 18 min in the training and testing, and the average prediction error is 2.69×10^{-4}. The time spent by the traditional SA algorithm, SVM, and the proposed method is listed in Table IV.

IV. Simulation and Measurement

The simulated and measured results of the three antennas obtained from the proposed method are given in this section. The photographs of the fabricated antennas are displayed in Fig. 7.

A. Reflection Coefficients

The simulated and measured reflection coefficients of the three antennas are shown in Fig. 8. It can be found that the measured results are in good agreement with the simulated ones. The simulated

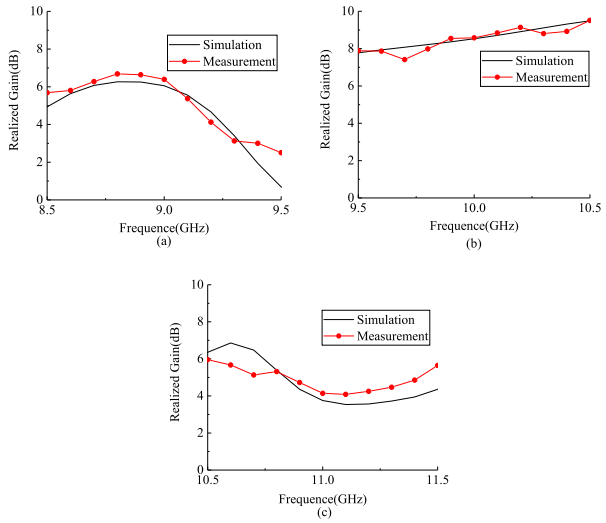

Fig. 12. Simulated and measured gains of (a) Antenna 1, (b) Antenna 2, and (c) Antenna 3.

center frequencies of the three antennas are 8.93, 10.1, and 11.1 GHz, respectively, while the measured results are 8.8, 9.85, and 11.2 GHz, respectively. Additionally, the simulated bandwidth of Antenna 1 is 23.2%, while those of Antenna 2 and Antenna 3 are 19.8% and 15.1%, respectively. The measured bandwidth of the three antennas are 31.8%, 17.3%, and 17.9%, respectively.

B. Radiation Patterns and Gains

In Figs. 9–11, the simulated and measured radiation patterns of the three antennas are given. For each antenna, radiation patterns of two frequencies in the working band are shown. It is observed that the simulated and measured results achieve a good agreement. In addition, in Fig. 12, the simulated and measured gains of three antennas are displayed. It can be found that the measured gains agree with the simulated ones.

V. Conclusion

In this communication, a hybrid method applying the ANN and the SA algorithm is proposed to design the wideband patch antenna with the required center frequency. The ANN could describe the nonlinear relationship between the geometric parameters and the EM responses of the antenna after ANN is trained well. The SA algorithm is used to broaden the bandwidth of the antenna with the required center frequency. More importantly, three sub-ANNs are applied to predict the EM responses of the antenna by data preprocessing. Thus, better results, faster training speed, and higher accuracy can be obtained when compared with the ANN trained by the dataset directly. Three wideband patch antennas with center frequencies of 8.93, 10.1, and 11.1 GHz are designed, simulated, and fabricated, respectively, to verify the proposed method. The calculated, simulated, and measured results agree well with each other, which proves that the proposed method is effective. The proposed method is promising to design wideband antennas.

References

[1] G.-N. Zhou, B.-H. Sun, Q.-Y. Liang, S.-T. Wu, Y.-H. Yang, and Y.-M. Cai, "Triband dual-polarized shared-aperture antenna for 2G/3G/4G/5G base station applications," *IEEE Trans. Antennas Propag.*, vol. 69, no. 1, pp. 97–108, Jan. 2021.

[2] S. Babu and G. Kumar, "Parametric study and temperature sensitivity of microstrip antennas using an improved linear transmission line model," *IEEE Trans. Antennas Propag.*, vol. 47, no. 2, pp. 221–226, Feb. 1999.

[3] Q. Xu, S. Zeng, F. Zhao, R. Jiao, and C. Li, "On formulating and designing antenna arrays by evolutionary algorithms," *IEEE Trans. Antennas Propag.*, vol. 69, no. 2, pp. 1118–1129, Feb. 2021.

[4] X. Liu et al., "Ultrabroadband all-dielectric transmitarray designing based on genetic algorithm optimization and 3-D print technology," *IEEE Trans. Antennas Propag.*, vol. 69, no. 4, pp. 2003–2012, Apr. 2021.

[5] Y.-F. Liu, L. Peng, and W. Shao, "An efficient knowledge-based artificial neural network for the design of circularly polarized 3-D-printed lens antenna," *IEEE Trans. Antennas Propag.*, vol. 70, no. 7, pp. 5007–5014, Jul. 2022.

[6] C. Cui, W. T. Li, X. T. Ye, Y. Q. Hei, P. Rocca, and X. W. Shi, "Synthesis of mask-constrained pattern-reconfigurable nonuniformly spaced linear arrays using artificial neural networks," *IEEE Trans. Antennas Propag.*, vol. 70, no. 6, pp. 4355–4368, Jun. 2022.

[7] J. Jin, C. Zhang, F. Feng, W. Na, J. Ma, and Q.-J. Zhang, "Deep neural network technique for high-dimensional microwave modeling and applications to parameter extraction of microwave filters," *IEEE Trans. Microw. Theory Techn.*, vol. 67, no. 10, pp. 4140–4155, Oct. 2019.

[8] Z. Liu, X. Hu, T. Liu, X. Li, W. Wang, and F. M. Ghannouchi, "Attention-based deep neural network behavioral model for wideband wireless power amplifiers," *IEEE Microw. Wireless Compon. Lett.*, vol. 30, no. 1, pp. 82–85, Jan. 2020.

[9] R. Hongyo, Y. Egashira, T. M. Hone, and K. Yamaguchi, "Deep neural network-based digital predistorter for Doherty power amplifiers," *IEEE Microw. Wireless Compon. Lett.*, vol. 29, no. 2, pp. 146–148, Feb. 2019.

[10] Q. Yang et al., "Transistor compact model based on multigradient neural network and its application in SPICE circuit simulations for gate-all-around Si cold source FETs," *IEEE Trans. Electron Devices*, vol. 68, no. 9, pp. 4181–4188, Sep. 2021.

[11] J. P. Jacobs, "Accurate modeling by convolutional neural-network regression of resonant frequencies of dual-band pixelated microstrip antenna," *IEEE Antennas Wireless Propag. Lett.*, vol. 20, no. 12, pp. 2417–2421, Dec. 2021.

[12] Z. Ž. Stankovic, D. I. Olcan, N. S. Doncov, and B. M. Kolundžija, "Consensus deep neural networks for antenna design and optimization," *IEEE Trans. Antennas Propag.*, vol. 70, no. 7, pp. 5015–5023, Jul. 2022.

[13] Q. Wu, H. Wang, and W. Hong, "Multistage collaborative machine learning and its application to antenna modeling and optimization," *IEEE Trans. Antennas Propag.*, vol. 68, no. 5, pp. 3397–3409, May 2020.

[14] L. Song, B. Zhang, D. Zhang, and Y. Rahmat-Samii, "Embroidery electro-textile patch antenna modeling and optimization strategies with improved accuracy and efficiency," *IEEE Trans. Antennas Propag.*, vol. 70, no. 8, pp. 6388–6400, Aug. 2022.

[15] D. Chen, X. Li, and S. Li, "A novel convolutional neural network model based on beetle antennae search optimization algorithm for computerized tomography diagnosis," *IEEE Trans. Neural Netw. Learn. Syst.*, vol. 34, no. 3, pp. 1418–1429, Mar. 2023.

[16] M. Sabbaghi, J. Zhang, and G. W. Hanson, "Machine learning target count prediction in electromagnetics using neural networks," *IEEE Trans. Antennas Propag.*, vol. 70, no. 8, pp. 6171–6183, Aug. 2022.

[17] C. Cui, W. T. Li, X. T. Ye, P. Rocca, Y. Q. Hei, and X. W. Shi, "An effective artificial neural network-based method for linear array beampattern synthesis," *IEEE Trans. Antennas Propag.*, vol. 69, no. 10, pp. 6431–6443, Oct. 2021.

[18] L.-Y. Xiao, W. Shao, F.-L. Jin, and B.-Z. Wang, "Multiparameter modeling with ANN for antenna design," *IEEE Trans. Antennas Propag.*, vol. 66, no. 7, pp. 3718–3723, Jul. 2018.

[19] L.-Y. Xiao, W. Shao, F.-L. Jin, B.-Z. Wang, and Q. H. Liu, "Inverse artificial neural network for multiobjective antenna design," *IEEE Trans. Antennas Propag.*, vol. 69, no. 10, pp. 6651–6659, Oct. 2021.

[20] X. Wang, K. Konno, and Q. Chen, "Diagnosis of array antennas based on phaseless near-field data using artificial neural network," *IEEE Trans. Antennas Propag.*, vol. 69, no. 7, pp. 3840–3848, Jul. 2021.

[21] T. N. Kapetanakis, I. O. Vardiambasis, M. P. Ioannidou, and A. Maras, "Neural network modeling for the solution of the inverse loop antenna radiation problem," *IEEE Trans. Antennas Propag.*, vol. 66, no. 11, pp. 6283–6290, Nov. 2018.

[22] L. Yuan, X.-S. Yang, C. Wang, and B.-Z. Wang, "Multibranch artificial neural network modeling for inverse estimation of antenna array directivity," *IEEE Trans. Antennas Propag.*, vol. 68, no. 6, pp. 4417–4427, Jun. 2020.